

Two-Dimensional Simulation Model for Contour Basin Layouts in Southeast Australia. I: Rectangular Basins

Manoj Khanna¹; Hector M. Malano, A.M.ASCE²; John D. Fenton³; and Hugh Turrall⁴

Abstract: Contour basin irrigation layouts are used to irrigate rice and other cereal crops on heavy cracking soils in Southeast Australia. In this study, a physically based two-dimensional simulation model that incorporates all the features of contour basin irrigation systems is developed. The model's governing equations are based on a zero-inertia approximation to the two-dimensional shallow water equations of motion. The equations of motion are transformed into a single nonlinear advection–diffusion equation in which the friction force is described by Manning's formula. The empirical Kostiakov equation and the quasi-analytical Parlange equation are used to model the infiltration process. The governing equations are solved by using a split-operator approach. The numerical procedure described here is capable of modeling rectangular basins; a procedure for irregular shaped basins is presented in Paper II. The model was validated against field data collected on commercial lasered contour layouts.

DOI: 10.1061/(ASCE)0733-9437(2003)129:5(305)

CE Database subject headings: Basins; Australia; Two-dimensional flow; Simulation models; Irrigation.

Introduction

80% of Australia's national irrigated area is located in the Murray–Darling Basin, which covers parts of New South Wales, Victoria, Queensland, and South Australia. The Murray–Darling Basin located in the southeast of Australia covers 1,061,469 km², equivalent to 14% of the country's total area. Irrigated agriculture in Australia has resulted in substantial benefits to individual rural communities and the nation as a whole. It accounts for 28% of the total value of all agricultural production in Australia and contributes one third of the national output from rural industries by producing most of Australia's dairy products, cotton, rice, fruit, vegetables, and wine.

Contour basin irrigation layouts are used to irrigate rice in heavy soils in the Murray–Darling River basin in southeastern Australia. Most of the rice cultivation in Australia is done on these layouts, which are found in the states of New South Wales, Victoria, and Queensland. Approximately half of the irrigated land of southern New South Wales is developed under contour basin irrigation systems. They are used primarily on soils that have very low infiltration rates. Contour basin layouts in south-

east Australia exhibit particular features which distinguish them from similar forms of irrigation elsewhere in the world.

In these layouts, water is applied to group of multiple basins divided by check banks constructed across the slope. These are made by borrowing soil from the basin resulting in a toe-furrow along the banks. The basins are filled to the desired depth of water, which is retained until it infiltrates into the soil. The excess water is drained back into the supply channel and into the next basin. A typical layout of a contour basin irrigation system is shown in Fig. 1. The water flow patterns during inflow/advance and recession/outflow are shown in Figs. 2 and 3.

Contour layouts are designed and used for cultivation of rice where ponding of water is required. Due to shortage of irrigation water, the recent cap on water allocation in the Murray–Darling basin, and growing concern about the environmental impacts of waterlogging and salinity, the agriculture department in the area promotes crops with low irrigation requirements to be grown in rotation with rice to minimize adverse impacts on the environment and ground water. Crop rotation will also help improve the soil structure and organic matter and will ultimately enhance the water use efficiency without affecting the net income of the farmers.

Old layouts are inefficient when used with crops other than rice which do not require ponding of water. This is due to poor drainage from the basin leading to overirrigation, groundwater accession, and poor productivity. Similar problems of poor drainage also occur with rice cultivation when basins must be drained during the maturing stage prior to harvest.

Since rice has been traditionally grown on these soils with low permeability it is vital to introduce management flexibility that enables farmers to grow other crops on the same layouts that will yield better returns and will provide an alternate management option. However, existing practices for upgrading contour layouts are guided only by experience and intuitive understanding.

Overseas criteria and experience are not applicable to these situations as upland crops are not irrigated on contour irrigation systems. Basin irrigation systems used in other countries are usu-

¹Senior Scientist, Water Technology Centre, Indian Agricultural Research Institute, New Delhi 110012, India. E-mail: mkhanna@iari.res.in

²Associate Professor, Dept. of Civil & Environmental Engineering, University of Melbourne, Victoria 3010, Australia. E-mail: h.malano@devtech.unimelb.edu.au.

³Professor, Dept. of Civil & Environmental Engineering, Univ. of Melbourne, Victoria 3010, Australia. E-mail: fenton@unimelb.edu.au

⁴Senior Researcher, International Water Management Institute, P.O. Box 2075, Colombo, Sri Lanka. E-mail: h.turrall@cgiar.org

Note. Discussion open until March 1, 2004. Separate discussions must be submitted for individual papers. To extend the closing date by one month, a written request must be filed with the ASCE Managing Editor. The manuscript for this paper was submitted for review and possible publication on November 27, 2001; approved on January 8, 2003. This paper is part of the *Journal of Irrigation and Drainage Engineering*, Vol. 129, No. 5, October 1, 2003. ©ASCE, ISSN 0733-9437/2003/5-305–316/\$18.00.

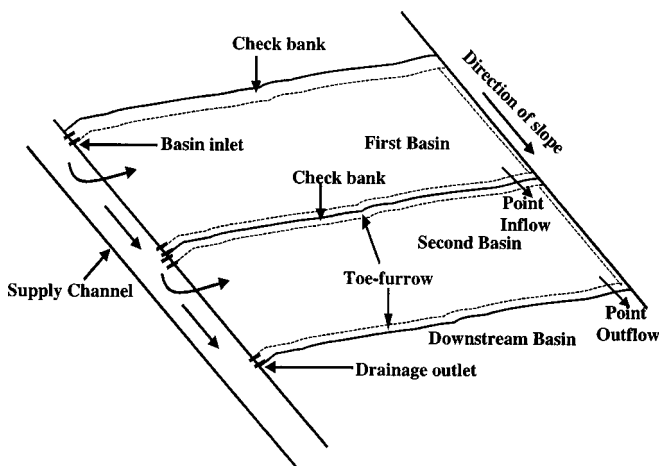


Fig. 1. Typical layout of contour basin irrigation system

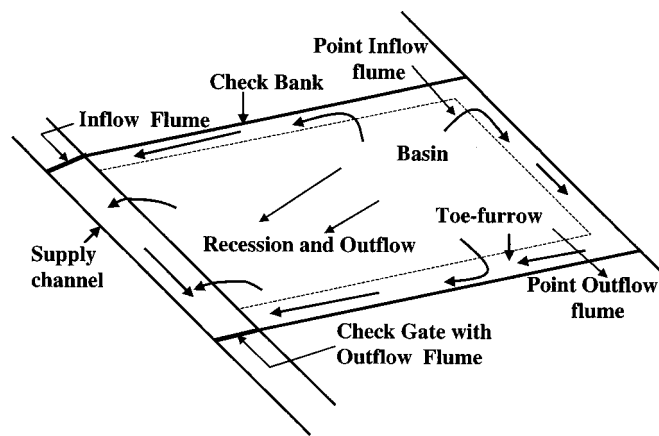


Fig. 3. Water flow pattern in contour basin layouts during recession and outflow

ally of single closed basins, which are independent of each other and not hydraulically connected.

There are many design parameters which influence hydraulic processes during an irrigation event in contour basin layouts. It is very difficult to predict and compare the performance of alternative design layouts without using a physically based simulation model to describe the process. The development of design guidelines and benchmarks for contour basin layouts can only be simulated by modeling all the hydraulic processes involved in an irrigation event. This paper describes a two-dimensional simulation model designed to evaluate the performance of existing layouts and to provide a design tool that can be used for design of new layouts and developing general guidelines for design and management of contour basin layouts.

Model

The design and management of contour basin layouts for rice and nonrice crops requires detailed knowledge of the hydraulics of overland flow, infiltration, and drainage behavior. Several two-dimensional mathematical models have been developed for simulation of overland flow conditions in basin irrigation (Playan et al. 1994a; Strelkoff et al. 1996; Singh and Bhallamudi 1997). Playan

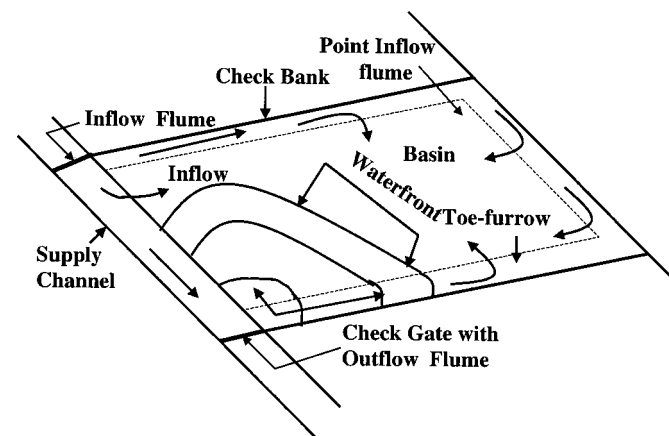


Fig. 2. Water flow pattern in contour basin layouts during inflow and advance

et al. (1994a,b) and Singh (1996) developed two-dimensional basin irrigation models based on shallow water equations using the Kostikov–Lewis equation to describe infiltration. Strelkoff et al. (1996) developed their simulation model based on a zero-inertia approximation of the two-dimensional shallow water equations. These models are used for individual closed basins in which drainage from the basin is ignored. Moreover none of these models is able to describe typical contour basin systems with the peculiar characteristics of those found in Southeast Australia such as presence of toe-furrows, irregular shapes, and multiple basin operation involving outflow from one basin to another through the check banks and backflow into the supply channel.

In this study, a two-dimensional simulation model for contour basin irrigation is developed. The model is based on the zero-inertia approximation of the Saint–Venant Equations (Chaudhry 1993). In this model, the equations are transformed into a single nonlinear advection–diffusion equation, in which friction forces are described using the Manning equation, and infiltration is described using the empirical Kostikov–Lewis equation or the quasi-analytical Parlange equation.

There are many finite-difference and finite-element methods available for solving nonlinear equations, but most are plagued by the difficulty in approximating both the advective and diffusive terms of the equation with comparable accuracy (Holly and Usseglio-Polatera 1984). One way of obtaining acceptable accuracy is by solving the advection and diffusion terms using different methods for each, in a “split-operator” approach. Under this approach, advection is solved using a characteristic method whose favourable performance in one and two dimensions has been demonstrated (Holly and Preissmann 1977; Glass and Rodi 1982; Holly and Usseglio-Polatera 1984). The method of approximation of the advection component is accurate when combined with appropriate cubic spline interpolation (Schohl and Holly 1991). Here a cubic spline interpolation is used with the method of characteristics and also for the diffusion component. This approach provides an alternative to the existing methods for advection–diffusion type equations with nearly the same accuracy while improving the efficiency of the solution.

This paper deals with the numerical scheme used for the solution of governing equations with regular (rectangular) grid discretisations. The model is capable of dealing with point or linear water inflow and several simultaneous inlet points. The model is also capable of describing the drainage runoff from one basin to an adjacent one. Field experiments were conducted on a commer-

cial layout to assess the performance of the existing system and to validate the models. However, a different numerical scheme was developed for irregular field shapes and multiple basin operation and is presented in Paper II by Khanna et al. (2003).

Governing Equations

Overland flow is described by the depth-averaged flow equations (Chaudhry 1993). These equations in hydrodynamic form consist of the continuity equation and the momentum equation. The two-dimensional continuity equation for shallow water flow is written as

$$\frac{\partial H}{\partial t} + \frac{\partial q_x}{\partial x} + \frac{\partial q_y}{\partial y} + I_s = 0 \quad (1)$$

where $q_x = uh$ and $q_y = vh$, discharge per unit width (m^2/s) in the x and y directions respectively; h = water depth (m); u and v = velocities in the x and y directions (m/s); $H = h + z_0$ = water surface elevation above the datum; z_0 = bottom elevation above datum (m); I_s = volumetric rate of infiltration rate per unit area (m/s); and t = time (s).

The momentum equations for shallow overland flow can be simplified by neglecting the inertial terms. The effect of these terms becomes small compared with those describing the effect of gravity and friction in shallow water flow situations. This is typical of agricultural fields, where velocities are low due to high vegetation resistance, small depths (high relative roughness), flat slope and low discharge. The momentum equations in the x and y directions after neglecting inertial terms are given by

$$\frac{\partial H}{\partial x} + S_{fx} = 0 \quad (2)$$

$$\frac{\partial H}{\partial y} + S_{fy} = 0$$

where S_{fx} and S_{fy} = components of friction slope in the x and y directions. Now the Manning equation is used to relate the discharge vector to the head gradient (negative of friction slope). In one-dimensional uniform flow, the discharge q is described by the Manning equation as follows:

$$q = \frac{1}{n} h^{5/3} S_f^{1/2} \quad (3)$$

where n = Manning roughness coefficient; and S_f = friction slope. The discharge vector per unit width in x and y directions can be generalized as follows:

$$q_x = q \cos \theta \quad (4)$$

$$q_y = q \sin \theta$$

where $\theta = \tan^{-1}(q_y/q_x)$ = angle between the flow direction and positive x direction. In diffusion flow, the friction slope is assumed to be equal to the slope of water surface, and is calculated as

$$S_f = \sqrt{\left(\frac{\partial H}{\partial x}\right)^2 + \left(\frac{\partial H}{\partial y}\right)^2} \quad (5)$$

The discharge components in the x and y directions can be obtained by combining Eqs. (2), (3), (4), and (5) which yield

$$q_x = -\frac{1}{n} \frac{(H-z_0)^{5/3}}{\left[\left(\frac{\partial H}{\partial x}\right)^2 + \left(\frac{\partial H}{\partial y}\right)^2\right]^{1/4}} \cdot \frac{\partial H}{\partial x} \quad (6)$$

$$q_y = -\frac{1}{n} \frac{(H-z_0)^{5/3}}{\left[\left(\frac{\partial H}{\partial x}\right)^2 + \left(\frac{\partial H}{\partial y}\right)^2\right]^{1/4}} \cdot \frac{\partial H}{\partial y}$$

The overland flow equations can now be transformed into a single nonlinear advection–diffusion equation by substituting the q_x and q_y from Eq. (6) into the mass conservation Eq. (1), and solving by differentiating and separating the coefficients of the time derivative, the first, second, and mixed spatial derivatives of H yields

$$\frac{\partial H}{\partial t} + U \frac{\partial H}{\partial x} + V \frac{\partial H}{\partial y} = D_{11} \frac{\partial^2 H}{\partial x^2} + D_{12} \frac{\partial^2 H}{\partial x \partial y} + D_{22} \frac{\partial^2 H}{\partial y^2} - I_s \quad (7)$$

where U and V are given by

$$U = -\frac{5}{3n} \frac{(H-z_0)^{2/3}}{\left[\left(\frac{\partial H}{\partial x}\right)^2 + \left(\frac{\partial H}{\partial y}\right)^2\right]^{1/4}} \left(\frac{\partial H}{\partial x} - \frac{\partial z_0}{\partial x}\right) \quad (8)$$

$$V = -\frac{5}{3n} \frac{(H-z_0)^{2/3}}{\left[\left(\frac{\partial H}{\partial x}\right)^2 + \left(\frac{\partial H}{\partial y}\right)^2\right]^{1/4}} \left(\frac{\partial H}{\partial y} - \frac{\partial z_0}{\partial y}\right) \quad (9)$$

Eq. (7) describes two-dimensional overland flow in advection–diffusion form including infiltration. The left-hand side of the equation is the advection component in which U and V are advection velocities. The right-hand side is the diffusion component with D_{11} , D_{12} , and D_{22} as diffusion coefficients. This is similar to the advection–diffusion equation for scalar transport. Infiltration is considered as a sink term on the right hand side of the equation.

The diffusion coefficients D_{11} , D_{12} , and D_{22} are given by

$$D_{11} = \frac{(H-z_0)^{5/3}}{n} \frac{\frac{1}{2} \left(\frac{\partial H}{\partial x}\right)^2 + \left(\frac{\partial H}{\partial y}\right)^2}{\left[\left(\frac{\partial H}{\partial x}\right)^2 + \left(\frac{\partial H}{\partial y}\right)^2\right]^{5/4}} \quad (10)$$

$$D_{12} = -\frac{(H-z_0)^{5/3}}{n} \frac{\frac{\partial H}{\partial x} \frac{\partial H}{\partial y}}{\left[\left(\frac{\partial H}{\partial x}\right)^2 + \left(\frac{\partial H}{\partial y}\right)^2\right]^{5/4}} \quad (11)$$

$$D_{22} = \frac{(H-z_0)^{5/3}}{n} \frac{\left(\frac{\partial H}{\partial x}\right)^2 + \frac{1}{2} \left(\frac{\partial H}{\partial y}\right)^2}{\left[\left(\frac{\partial H}{\partial x}\right)^2 + \left(\frac{\partial H}{\partial y}\right)^2\right]^{5/4}} \quad (12)$$

Overland Flow in Toe-Furrow

Contour basins have a toe-furrow on three sides. Flow into contour basins enters and exits through the toe-furrows. Flow in the toe-furrow needs special treatment, as the toe-furrow is completely filled long before the interior of the basin. The depth and cleanliness of the toe-furrow was observed to significantly affect the rate of flow at which water advances over the surface of the

basin. The flow depth in the toe-furrow can thus be considered to act as a boundary to overland flow from which water advances over the basin. In this study, flow in the toe-furrow is treated separately from the interior of the basin as one-dimensional flow with infiltration.

The derivation of the one-dimensional flow equation for the toe-furrow is the same as that of Eq. (7) for two-dimensional overland flow. The advantage of using the same form of equation is that it can be solved using the same numerical scheme used for the two-dimensional case.

Infiltration

Two alternative infiltration equations, namely Kostiakov–Lewis and Parlange equations are used to describe infiltration in the model.

Kostiakov–Lewis Equation

Many of the earlier surface irrigation models (Clemmens et al. 1981; Playan et al. 1994a,b; Singh and Bhallamudi 1997) have described infiltration using empirical equations, in particular the modified Kostiakov (1932) equation. The present model also incorporates the empirical infiltration equation given by Kostiakov–Lewis (Clemmens et al. 1981; Playan et al. 1994a). Empirical parameters for this equation are available for some soil types. Furthermore, this equation is easy to incorporate into the simulation model and imposes low computational overhead.

This equation is given by

$$Z = kt_{op}^a + bt_{op} \quad (13)$$

where Z = cumulative infiltration volume per unit area (m); a , k , b = empirical constants; and t_{op} = intake opportunity time, or the time since the wetting front arrived at the point or node in consideration. The infiltration rate can be determined by differentiating Eq. (13) with respect to intake opportunity time

$$I_s = \frac{dZ}{dt} = akt_{op}^{a-1} + b \quad (14)$$

where I_s = volumetric rate of infiltration per unit area (m/s).

Parlange Equation

Infiltration can also be described using the quasianalytical Parlange with three soil characteristic parameters. These parameters are sorptivity S , hydraulic conductivity parameter K_1 , and a shape parameter δ which is related to hydraulic conductivity of the soil (Parlange et al. 1982). Sorptivity S is related to soil water diffusivity. The second parameter, $K_1 = K_s - K_i$, is the difference between the hydraulic conductivity (m/s) at saturation (soil moisture $\theta = \theta_s$), and the hydraulic conductivity (m/s) at uniform initial moisture content (soil moisture $\theta = \theta_i$).

This equation was further modified, by Haverkamp et al. (1990), by introducing an additional parameter h_{str} , that takes into account the possibility of an infinite diffusivity near saturation. This is the minimal soil pressure value in the wetting cycle at which a continuous nonwetting phase exists in the porous medium. h_{str} is constant in time and independent of the changing boundary condition values. This equation is reformulated through differentiation and then analytically integrated to obtain an equation in terms of intake opportunity time with an assumption of constant positive head over time (Edenhofer and Schmitz 1985; Schmitz et al. 1985; Singh 1996) to yield

$$t_{op} = \frac{S^2 + 2h_{str}K_s(\theta_s - \theta_i)}{2\delta(1-\delta)(K_s - K_i)^2} \ln \left[1 + \delta \frac{K_s - K_i}{I_s - K_i} \right] + \frac{K_s(h - h_{str})(\theta_s - \theta_i)}{(K_s - K_i)(I_s - K_s)} + \left[\frac{S^2 + 2h_{str}K_s(\theta_s - \theta_i) + 2(1-\delta)K_s(h - h_{str})(\theta_s - \theta_i)}{2(1-\delta)(K_s - K_i)^2} \right] \times \ln \left(\frac{I_s - K_s}{I_s - K_i} \right) \quad (15)$$

in which θ_i = initial soil moisture at the point; θ_s = saturated soil moisture content; S = sorptivity (m/\sqrt{s}); h_{str} = minimum soil moisture pressure-head value in the wetting cycle (m); and δ = shape parameter is an indicator of the variation of hydraulic conductivity with the soil moisture content and is given by the relation

$$\delta((\theta_s - \theta_i)(K_s - K_i)) = \int_{\theta_i}^{\theta_s} (K_s - K_i) d\theta \quad (16)$$

Eq. (15) can be used to determine infiltration rate I_s by iteration for a given intake opportunity time, depth of flow h and other soil parameters. Depth of flow h is considered to be invariant with time for the purpose of calculating infiltration rate (during each time step).

Numerical Scheme

The two-dimensional model formulated in this study is based on the analytical description of the following processes:

1. Surface flow governing equations by a single advection–diffusion equation, and
2. Subsurface flow described either by the Kostiakov–Lewis infiltration model or the quasianalytical physically based Parlange model.

The advection–diffusion equation considers the combined effect of the advection and diffusion processes, which describe the physical transport of mass. The solution of this equation can be performed in two separate stages for the advection terms assuming there is no diffusion and then the diffusion terms. This is known as the “split-operator” approach, in which advection and diffusion are computed independently over short time increments (Komatsu et al. 1985).

The advantage of the split-operator approach is that it allows the use of an accurate scheme for each process (Komatsu et al. 1997). This approach also helps to exploit the advantage of the hyperbolic nature of the advection–diffusion equation to devise characteristic-based numerical schemes which allow natural treatment of boundary conditions and provide a framework for a simple and accurate methodology (Komatsu et al. 1985). Using this approach, the solution is obtained in two steps. The results from the first or intermediate step for solving the advection terms are added to the diffusion terms based on the values obtained for the advection term.

Various numerical schemes can be used for the solution of the advection and diffusion components. These schemes depend on the form of discretization of the physical domain in either regular grid (rectangular) or quadrilateral grid (irregular). In this study, regular grid discretization is used for contour basins of regular shape, while quadrilateral or irregular discretization is used for basins of irregular shape. (A model for irregular shaped basins is presented in Paper II; see Khanna et al. 2003.)

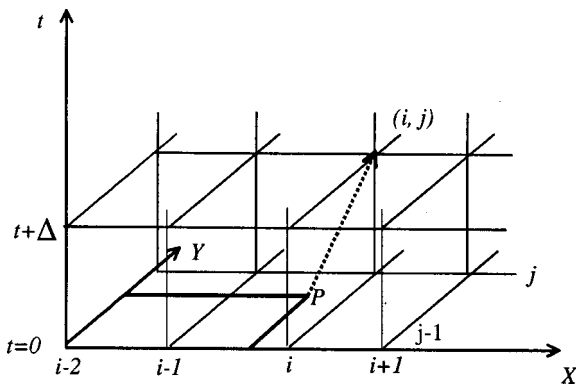


Fig. 4. Discretization of solution domain (rectangular grid)

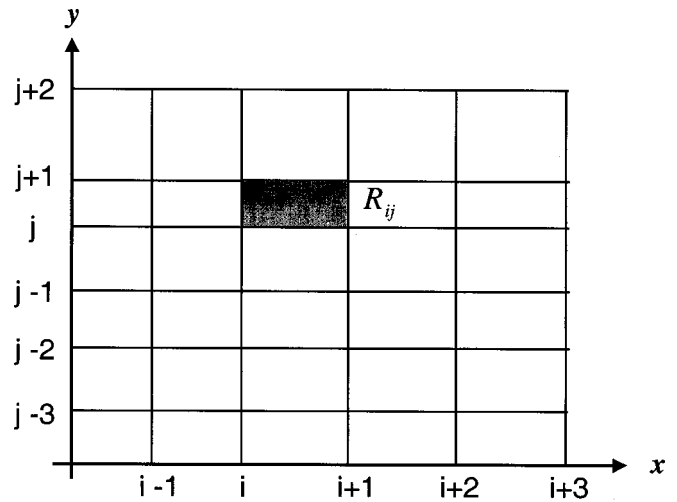


Fig. 5. Computational domain for bicubic splines

Solution of Advection Term

The choice of method for the solution of the advection component is the method of characteristics described by several earlier authors (Holly and Preissmann 1977; Glass and Rodi 1982; Holly and Usseglio-Polatera 1984; Holly and Toda 1985; Komatsu et al. 1985; Komatsu et al. 1997). In this method, neglecting all the terms on the right hand side of Eq. (7) yields the following advection equation:

$$\frac{\partial H}{\partial t} + U \frac{\partial H}{\partial x} + V \frac{\partial H}{\partial y} = 0 \quad (17)$$

This equation states that the scalar quantity H of a given fluid particle does not change along the flow pathline. Such a pathline is actually a characteristic line for Eq. (17), and its direction at any point in the flow domain is given by the following ordinary differential equations:

$$\begin{aligned} \frac{dx}{dt} &= U(x, y, t) \\ \frac{dy}{dt} &= V(x, y, t) \end{aligned} \quad (18)$$

The characteristic equation that holds along any one of these lines is

$$\frac{dH}{dt} = 0 \quad (19)$$

The solution is carried out by replacing Eq. (17) with the ordinary differential Eqs. (18) and (19), which are then integrated numerically over a space-time grid. The location of the characteristic lines on a rectangular grid is shown in Fig. 4.

The characteristic line starts at point P and extends to the node denoted by (i, j) . The solution of H after advection is given by

$$H^*(x_i, y_j, t + \Delta) = H(x_i - U_{i,j}\Delta, y_j - V_{i,j}\Delta, t) \quad (20)$$

where Δ = time step. Eq. (20) shows that the advected value of H is equal to the value of H previously at $(x_i - U_{i,j}\Delta, y_j - V_{i,j}\Delta, t)$.

This implies that if the location of point P (origin of the characteristic line) at the old time step has been found, the solution of the advection equation can be completed by determining the value of H at that point. The key to the characteristic solution, then, is the accurate interpolation of the internodal values. Holly and Preissmann (1977) used the method of characteristics in conjunction

with Hermite bicubic interpolation to solve the advection part of the transport equation with minimum numerical damping or oscillations. They carried out the interpolation using, not only concentration at two nearby points, but also the spatial derivatives there. This gave good results with fourth-order accuracy in a one-dimensional scalar transport problem. Glass and Rodi (1982) modified and extended this method to two-dimensions for simulation of scalar mass transport. Holly and Komatsu (1983) also modified Holly and Preissmann's (1977) two-point fourth order method to an eight-point method. This method had some practical difficulties in its general implementation (Komatsu et al. 1985) because each interpolation was based on 64 adjacent points resulting in an overly cumbersome scheme.

Another way of interpolating H is to construct bicubic-spline-interpolating polynomials over the entire computational domain at the old time step. A bicubic spline polynomial, passes through each data point and is continuous in its zeroth, first, and second derivatives. Construction of the bicubic spline requires the solution of a linear algebraic system for the second derivatives through inversion of a tridiagonal matrix. Implicit in this construction is the imposition of the upstream and downstream boundary conditions for the second derivatives. Bicubic-spline-interpolating polynomials were constructed over the entire domain (Fig. 5) and used for the estimation of H at point P (Shikin and Plis 1995). The inner points in the computational domain are called knots of the grid. The bicubic spline function $F(x, y)$, over the entire domain, is defined by

$$F(x, y) = \sum_{p=0}^3 \sum_{q=0}^3 c_{p,q}^{(i,j)} (x - x_i)^p (y - y_j)^q \quad (21)$$

and in each cell

$$R_{ij} = \{(x, y) | x_i \leq x \leq x_{i+1}, y_j \leq y \leq y_{j+1}\}, \quad i = 0, 1, \dots, m, \quad j = 0, 1, \dots, n \quad (22)$$

where R_{ij} represents the entire computational domain. This satisfies the conditions

$$F(x_i, y_j) = w_{ij}, \quad i = 0, 1, \dots, m, \quad j = 0, 1, \dots, n \quad (23)$$

where w_{ij} = value of the function at each node; and $c_{p,q}^{(i,j)}$ = spline coefficients. 16 mn coefficients $c_{p,q}^{(i,j)}$ are needed to construct the bicubic spline. Eq. (23) provides $(m+1)(n+1)$ equations while additional equations are available in the form of re-

restrictions on the values of the spline derivatives at the boundary and corner knots of the grid. The boundary conditions used for this model require that the following derivatives of the desired spline be continuous on the lines $x=x_1$ and $x=x_{m-1}$:

$$\frac{\partial S}{\partial x}, \frac{\partial S}{\partial y}, \frac{\partial^2 S}{\partial x^2}, \frac{\partial^2 S}{\partial x \partial y}, \frac{\partial^2 S}{\partial y^2}, \frac{\partial^3 S}{\partial x^3}$$

$$\frac{\partial^3 S}{\partial x^2 \partial y}, \frac{\partial^3 S}{\partial x \partial y^2}, \frac{\partial^4 S}{\partial x^3 \partial y}, \frac{\partial^4 S}{\partial x^2 \partial y^2}, \frac{\partial^5 S}{\partial x^3 \partial y^2}$$

and the derivatives

$$\frac{\partial S}{\partial x}, \frac{\partial S}{\partial y}, \frac{\partial^2 S}{\partial x^2}, \frac{\partial^2 S}{\partial x \partial y}, \frac{\partial^2 S}{\partial y^2}, \frac{\partial^3 S}{\partial x^2 \partial y}$$

$$\frac{\partial^3 S}{\partial x \partial y^2}, \frac{\partial^3 S}{\partial y^3}, \frac{\partial^4 S}{\partial x^2 \partial y^2}, \frac{\partial^4 S}{\partial x \partial y^3}, \frac{\partial^5 S}{\partial x^2 \partial y^3}$$

be continuous on the lines $y=y_1$ and $y=y_{n-1}$. This is known as the “not-a-knot” condition (de Boor 1978). Under this condition, the value of the first and second partial derivatives of the desired function with respect to x and y need not to be specified on the boundary knots. A spline satisfying this condition has a greater than usual smoothness. Once the spline is constructed, its coefficients are used to interpolate the value of H at point P .

Solution of Diffusion Term

Nonadvection terms such as diffusion and sources or sinks should also be estimated in a way compatible with the numerical treatment of advection. The computation of diffusion in the split-operator approach can be accurately carried out using a variety of finite difference and finite element numerical schemes (Komatsu et al. 1997).

In this model, bicubic splines were again used for calculating the diffusion terms. The advantage of constructing bicubic splines is that they also enable the calculation of the second and mixed derivatives of the function which are required to determine the diffusion terms at the foot of the characteristic line. These are calculated at the foot of the characteristic line indicating that the calculation of the diffusion terms then proceeds along the characteristic line. This approach was found to improve stability. Second and mixed derivatives of H are calculated using bicubic splines.

Combining the advected values of H with the values of the second and mixed derivatives of H calculated using the bicubic splines with respect to x and y , the values of H at the new time step are calculated as

$$H_{i,j}(t+\Delta) \approx H_{i,j,t}^* + \Delta D_{11} \frac{\partial^2 H_{i,j}}{\partial x^2} + \Delta D_{12} \frac{\partial^2 H_{i,j}}{\partial x \partial y}$$

$$+ \Delta D_{22} \frac{\partial^2 H_{i,j}}{\partial y^2} - I_s \Delta \quad (24)$$

Initial and Boundary Conditions

The methodology used for the numerical solution is explicit in nature, requiring initial and boundary conditions. At $t=0$, a finite value of water depth H (Bed elevation + 10^{-8} m) is assigned at each node, to start the computation and avoid a numerical singularity. This method does not introduce significant errors (Playan et al. 1994a; Singh and Bhallamudi 1997). Infiltration depth is set to zero at all the nodes at time $t=0$. The land surface elevation, $z_0(x,y)$ is an initial condition and an input to the model.

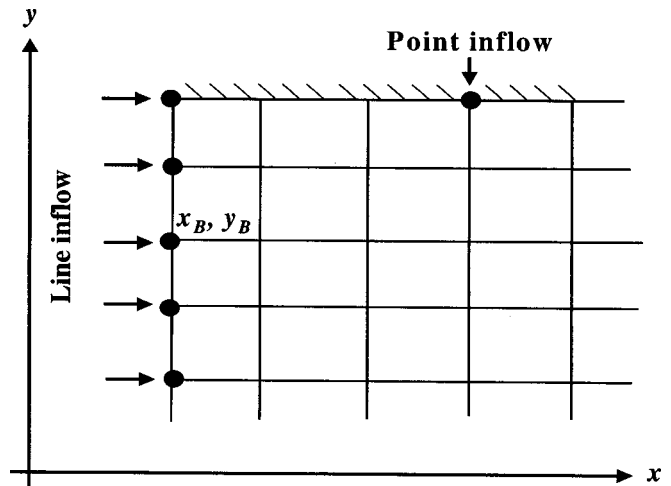


Fig. 6. Line and point inflow boundary

Inflow Boundary

A distinct feature of contour basin irrigation in Southeast Australia is that inflow to the basin occurs as overflow from the side supply channel as well as from the toe-furrows. Water first enters from the supply channel and into the toe-furrows, and once all the toe-furrows are filled water overflows onto the field.

In the computational scheme, the depth of water in the supply channel is considered to act as a boundary condition to the overland flow in the basin. In a multiple basin system, the depth of flow in the supply channel drops when the water supply is diverted onto the second basin upon completion of irrigation in the first basin. The depth of flow in the supply channel is thus imposed as a boundary condition during inflow to the basin as shown in Fig. 6. This is termed a line inflow boundary condition. The line inflow boundary condition is defined as a flow depth and specified as

$$H(x_B, y_B, t) = h(x_B, y_B, t) + z_0(x_B, y_B, t) \quad (25)$$

where $H(x_B, y_B, t)$ = water surface elevation at the boundary line-inflow node; $h(x_B, y_B, t)$ = depth of flow at the boundary line-inflow node; $z_0(x_B, y_B, t)$ = bed elevation at the same point; and x_B and y_B = values of x and y that define the location of these points on a fixed boundary. The model also incorporates the presence and effect of a toe-furrow along the basin check bank. The depth of flow in the toe-furrow acts as a flow boundary to the overland flow over the basin. The depth of flow in the toe-furrows is described by assuming one-dimensional flow and this condition is applied to three sides of the basin (two-side check banks and bottom check bank). The one-dimensional flow equation for toe-furrows is also solved using the “split-operator” approach.

Internal Boundary Condition

The solution of the overland flow problem in undulating basins causes mass balance errors due to varying soil surface elevations. The problem arises when a node is characterized by a bottom elevation higher than the water surface elevation in a neighboring node. In this case, flow would occur outward from the dry node, which is a physical impossibility. This problem causes errors in the estimation of final mass balance (Zapata and Playan 2000). This problem was reported by Strelkoff et al. (1996) who sug-

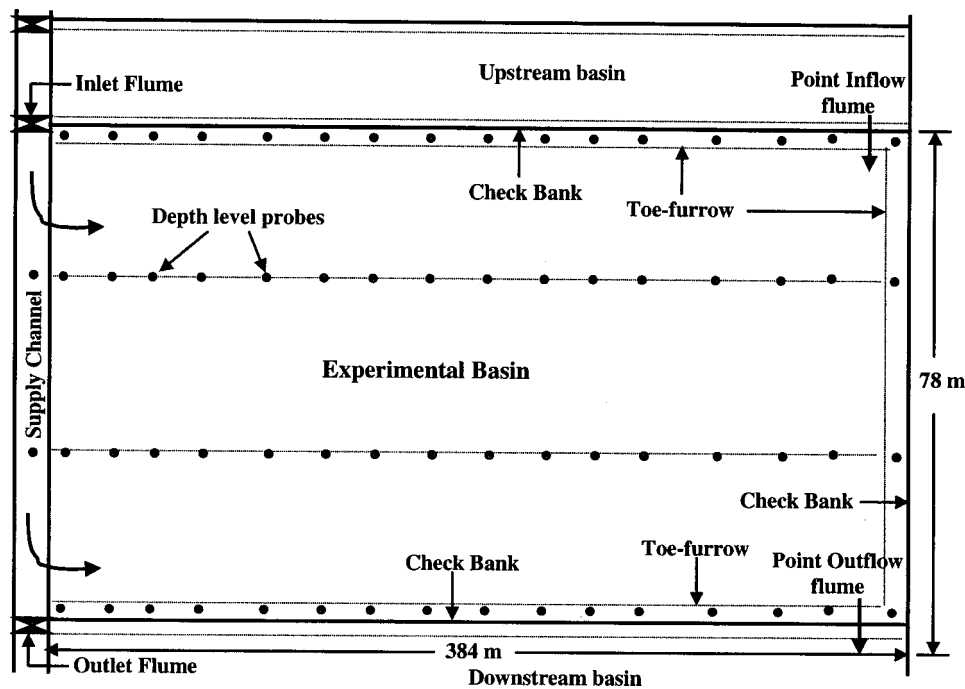


Fig. 7. Layout of single rectangular contour basin with line and point inflow

gested a procedure to overcome the problem by specifying an internal boundary condition as a practical means of dealing with an undulating basins surface. At each time step, the model checks dry and wet nodes (a wet node is defined as one with a minimum depth of 1 mm). If the water surface slopes away from a dry node the advected velocities and diffusion coefficients at that node are set to zero. This problem is more acute at nodes near the toe-furrow due to the difference in bed elevations.

Determining Infiltration

Infiltration in Eq. (24) is determined by using the empirical Kostikov–Lewis expression given by Eq. (14) or by the quasi-analytical Parlange Eq. (15). As the computation progresses, it is possible that when the advance front reaches a node, the calculated infiltrated depth could be larger than the depth of flow available or alternatively the wetting front may not yet have reached that node. Therefore a procedure is introduced that only allows infiltration to start when a node is wet, which is characterized by a flow depth equal or greater than 10^{-3} m. If the depth of flow at a wet node is less than the infiltrated depth, then flow depth is reset to 10^{-8} m to avoid computation of a negative flow depth. This procedure introduces a small mass balance error due to violation of the continuity equation. This mass balance error is minimized by equating the infiltration depth to the flow depth available at that node and determining the new intake opportunity time corresponding to this new infiltration depth by inversely solving the Kostikov–Lewis equation (Playan et al. 1994a; Singh and Bhallamudi 1997).

If Parlange's equation is used, a new intake opportunity time is calculated at a wet node for each time step using Eq. (15). The equation is then solved iteratively using a Newton–Raphson technique for a given value of h and intake opportunity time.

Model Validation

The computer model was validated using field data obtained from an experiment conducted on a commercial farm during the irriga-

tion season 1998–1999 at Wyanda, New South Wales, Australia. Field experiments were carried out with a side ditch layout (Fig. 7) in which detailed monitoring of waterfront during advance and recession, flow depth, inflow and outflow was carried out. Field and grid nodes were mapped using a global positioning system (GPS). The GPS was also used to monitor the advance of the waterfront over the field by regularly walking along the waterfront. Inflow and outflow were monitored using a flow meter installed in flumes in the supply channel and at the outlet points (Figs. 2 and 3). The rectangular experimental bay was 384 m long by 78 m wide ($\cong 3$ ha). The basin which was sown to subclover had been laser leveled in both directions about 5 years earlier although it still has local undulations due to movement of sheep and vehicles. The contour map of the field was obtained from a survey based on 12.8 m \times 12.5 m grid spacing. The basin was nearly dead level with slopes of about 0.013 and 0.065% along the length and width of the basin, respectively.

A combination of three sources of data were used to validate the model. These are:

1. Basin monitoring data including advance, recession and flow depth were collected during the actual field experiments on a commercial layout;
2. Infiltration and roughness parameters obtained from the literature on experiments conducted on similar soils in the vicinity of the experimental area (Maheshwari and Jayawardane 1992; Maheshwari and McMahon 1992; Hume 1993); and,
3. Basic soil characteristics data collected from the experimental basins.

It is important to note that no parameter in the model was calibrated during the validation process. Instead, the model was independently validated using that outlined above. The validation variables used were cumulative area wetted during advance, waterfront advance pattern, and advance water balance. The model using the Kostikov–Lewis infiltration equation was validated against field data collected from the first irrigation whereas the model using Parlange's quasianalytical infiltration equation was

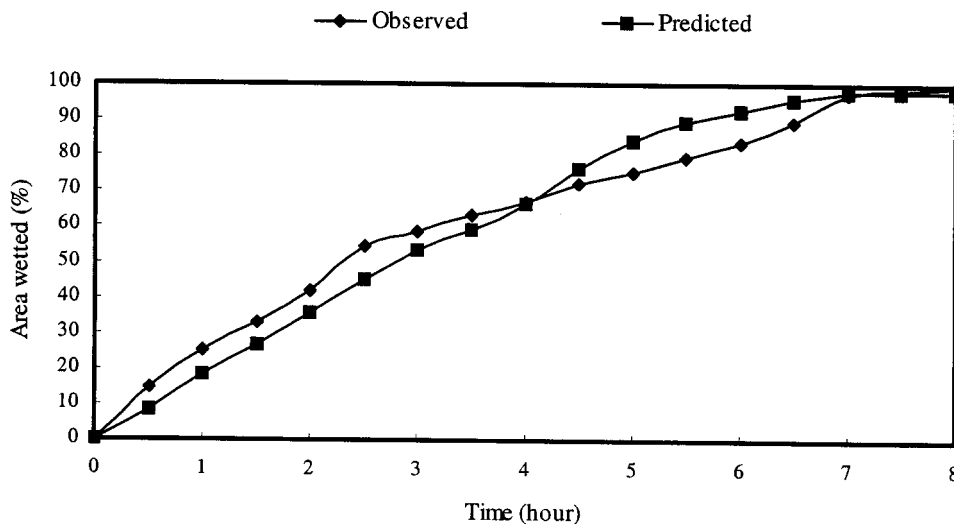


Fig. 8. Area wetted during advance for single rectangular contour basin with line inflow

validated against data collected during the second irrigation. The model validation was carried out using a 2 s time step which proved to yield the best model performance taking into account stability and accuracy.

Model Validation Using Kostiakov–Lewis Infiltration Equation

In the first irrigation, a contour basin with a toe-furrows on three sides and a supply channel was irrigated using line inflow from the side supply channel with an average discharge of 0.15 m³/s for 8.33 h (actual supply discharge varied from 0.12 to 0.18 m³/s). Outflow was allowed from the supply side of the basin into the supply channel after the inflow was cutoff.

The parameter of the Kostiakov–Lewis equation were taken as $k=0.055 \text{ m/s}^{0.026}$, $a=0.026$; and $b=3.0 \text{ mm/h}$. At the time of the experiment, the soil was completely dry and heavily cracked. Manning’s roughness coefficient was taken as 0.29 based on previous experimental results obtained from similar soil conditions (Maheshwari and McMahon 1992). Actual ground elevation data were used in the simulation. The contour basin was discretised on a 6.25 m×6.4 m grid in x and y directions, respectively, yielding a total of 806 nodes, 62 in the x direction and 13 in the y direction. The elevations of additional intermediate nodes were determined using linear interpolation of the observed data (only 217 node elevations were obtained during the survey of the field). The model was run for the total simulation time of 43 h until the lateral flow ceased. Recession was very slow as outflow was allowed only as backflow into the supply channel through the toe-furrows. In common practice farmers allow water to drain into the supply channel as well as into downstream basin through check gates located on the check bank. These gates are normally located near the inlet end of the basin.

Field monitoring of the recession was hampered by the furrowing effect of the tillage equipment, movement of sheep and small-scale topographical effects. These microtopography effects could not be accounted for with the grid spacing used for the discrete model.

Cumulative Area Wetted During Advance

Basin overland flow is a two-dimensional flow problem. In order to take this into account, model outputs were contrasted against

field observed advance data. Fig. 8 shows a comparison of area wetted during advance computed by the model and field observed data. It can be observed that the modeling results satisfactorily match the field observations. Variations between the observed and predicted data can be ascribed to spatial variation in topography caused by sheep and vehicle traffic, spatial variation in soil infiltration characteristics and the variation in actual inflow rates. The spatially varying factors are not accounted for by the model given that the discretization scale exceeds the scale of resolution required to account for these effects.

Waterfront Advance

Figs. 9 and 10 show the waterfront configuration obtained from the model and field observed advance at 2 and 4 h, respectively, during the advance phase with inflow occurring only from the supply channel. The direction of flow is from left to right. It can be observed from these figures that the waterfront advance simulated by the model matches satisfactorily with field data. These

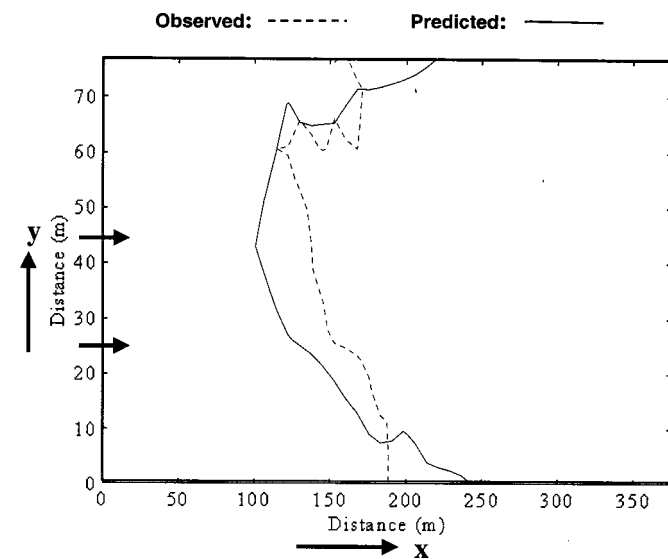


Fig. 9. Comparison of waterfront advance with model prediction after 2 h (arrows indicate direction of flow)

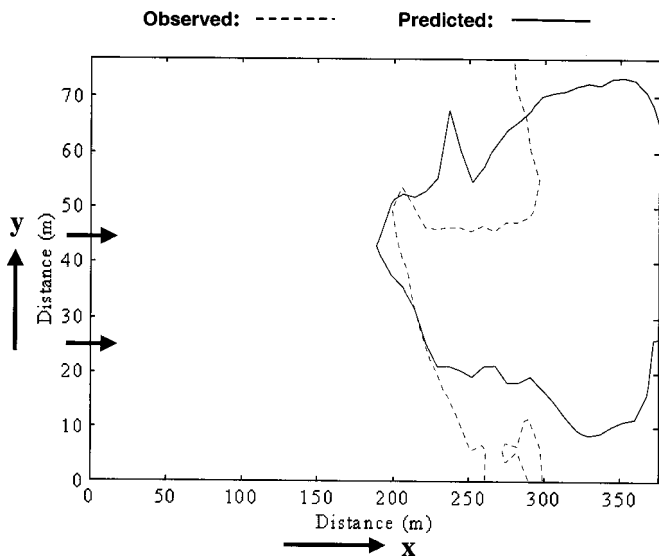


Fig. 10. Comparison of waterfront advance with model prediction after 4 h (arrows indicate direction of flow)

results indicate that the model has the capability of simulating the behavior of overland flow with satisfactory accuracy. These results the capacity of the model to simulate satisfactory accuracy using a line inflow boundary condition.

Advance Volume Balance

The comparison of water volume predicted from the model and observed in the field is shown in Fig. 11. The volume of water during advance obtained from the model is compared with the volume of inflow from the supply channel. The predicted volume of water during advance consists of overland volume and infiltrated volume. The absolute deviation between observed and predicted volume at the end of advance was about 8%. The main source of deviation can be attributed to the uniform infiltration parameters adopted for the whole basin as spatial variability of infiltration parameters was not considered in the present study.

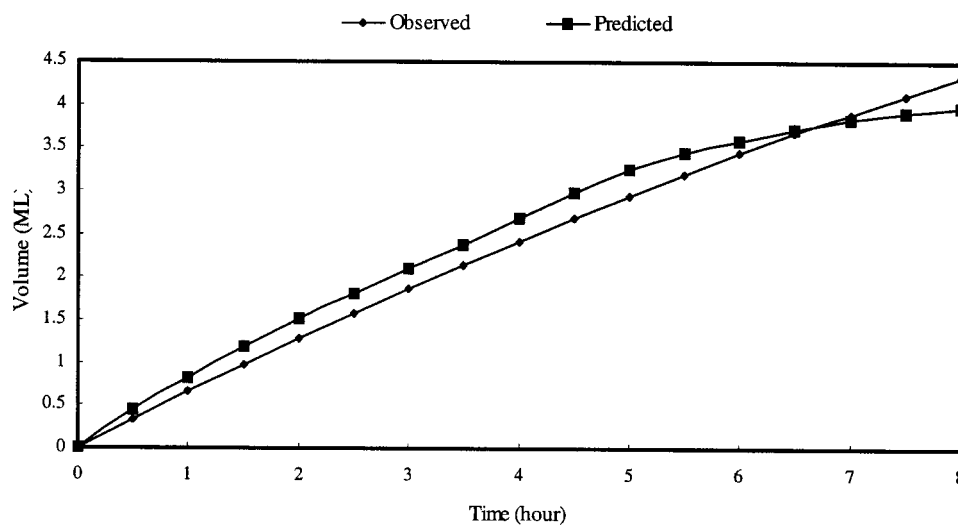


Fig. 11. Comparison of volume of water as predicted and observed during advance phase

Table 1. Values of Parameters of Parlange Infiltration Equation

Parameter	Value
θ_i	0.38
θ_s	0.47
K_i	5.67×10^{-16} m/s
K_s	2.29×10^{-6} m/s
S	2.64×10^{-4} m/ \sqrt{s}
δ	0.95
h_{str}	-0.02 m

Validation of Simulation Model Using Parlange Infiltration Equation

The quasianalytical Parlange infiltration equation is based on parameters depending on soil properties, depth of overland flow and time. The use of this equation requires the determination of soil saturated hydraulic conductivity, unsaturated hydraulic conductivity, initial and final volumetric soil moisture content, sorptivity and soil parameters δ and h_{str} . Some of these parameters were obtained by monitoring soil moisture before and after the irrigation event and measuring the basic soil properties in the laboratory and field. The values of initial and final soil moisture were measured during the field experiments. The values of other parameters such as unsaturated hydraulic conductivity K_i , saturated hydraulic conductivity K_s , and sorptivity S were drawn from a field monitoring study conducted on a similar soil in the experimental area (Smith 1999). The values of parameter δ and h_{str} suggested by Haverkamp et al. (1990) were used in the simulation. Table 1 shows a summary of all the equation parameters used in the computation of infiltration.

During the second irrigation of the season, the basin was irrigated from the side supply channel with an average discharge of $0.2 \text{ m}^3/\text{s}$ for 4 h. An additional point inflow (drainage runoff) from the upstream basin was also included. The average rate of the point inflow was taken as $0.025 \text{ m}^3/\text{s}$, which is the same as the value observed during the trial. After the inflow was cut off, outflow was allowed back into the supply channel and into the downstream basins through the check bank.

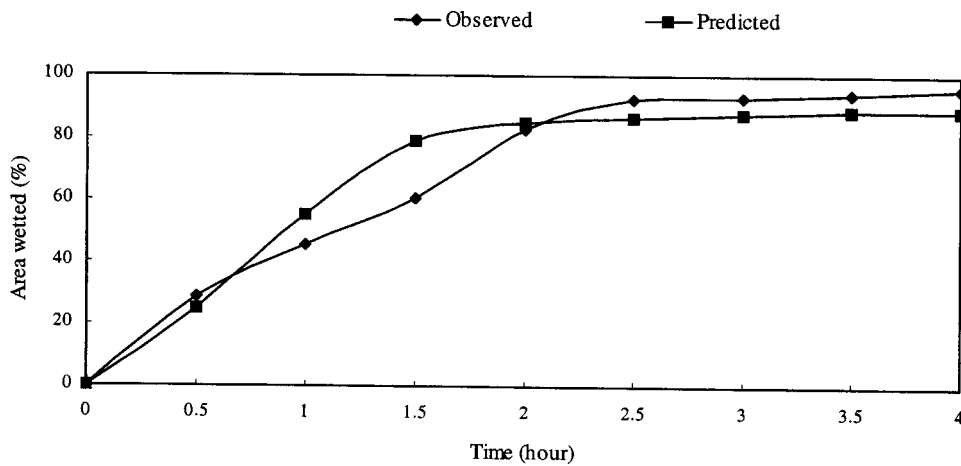


Fig. 12. Wetted area during advance for second irrigation using Parlange infiltration equation

Manning's coefficient for the simulation of this irrigation event was taken as 0.065 (Maheshwari and McMahon 1992) given that the soil was wet and all the cracks were closed indicating less resistance to flow compared to the first irrigation. The model was run for a total of simulation time of 24 h. Cumulative area wetted during advance, configuration of the waterfront advance and advance water balance obtained from the model simulation were used against field observed data to test model accuracy.

Cumulative Area Wetted During Advance

Fig. 12 shows the comparison of wetted area during advance obtained from field observations and modeling results using the Parlange infiltration equation. It can be observed that the model results compare well with the experimental data. The error in predicting the cumulative time employed to cover the basin area after completion of the advance phase is 7%. Deviations in the trajectory of wetted area prediction are due to the same reasons mentioned earlier such as soil variability, minor topographic undulations, spatial variability of infiltration and the variation in actual inflow rates which cannot be accounted for in the model.

Waterfront Advance

Figure 13 shows the waterfront advance pattern obtained from the simulation model using Parlange infiltration equation after 30 min of elapsed time. This run also incorporates inflow from the supply channel (line inflow) and drainage runoff from the upstream basin (point inflow). The direction of flow of water for line inflow was from left to right as indicated in Fig. 13.

The modeling results obtained with the Parlange's infiltration equation compare well with the observed pattern of waterfront advance. These results also indicate that the model is capable of incorporating drainage runoff inflow from the upstream basin which starts at the same time as inflow from the supply channel.

Advance Volume Balance

Fig. 14 shows the observed water balance during the advance phase and that predicted by the model using Parlange infiltration equation. The cumulative volume of water during advance predicted by the model shows good agreement for the whole of the advance phase. This good accuracy of prediction can be attributed

to the fact that Parlange infiltration equation includes the effect of surface flow depth which is an important factor once water has reached a point in the field and depth begins to increase and later recede over time. It has been shown in earlier surface irrigation models (Singh 1996) that for different values of sorptivity S and saturated hydraulic conductivity K_s , the inclusion of surface flow depth in the infiltration calculation affects the overall irrigation simulation results.

The inclusion of flow depth alters the overall water balance more significantly that it does the advance trajectory. Therefore, it appears to be important to include the effect of flow depth h on the infiltration prediction while simulating irrigation. One disadvantage of using Parlange equation is a fivefold increase in computation time due to the iterative method used to calculate depth of infiltration using a Pentium-II-333 MHz based personal computer. With the availability of faster personal computers, this disadvantage becomes less significant.

Figs. 12–14 indicate that the simulation model using the Parlange infiltration equation is capable of simulating the various phases of an irrigation event with satisfactory accuracy. The use

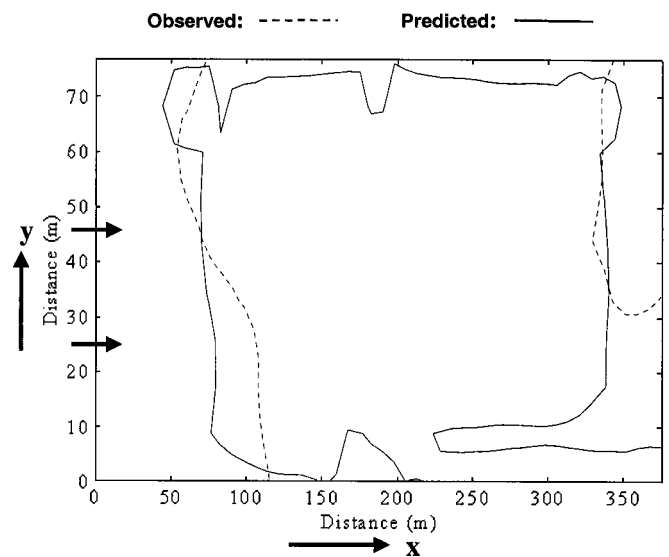


Fig. 13. Waterfront advance pattern after 30 min during second irrigation (arrows indicate direction of flow)

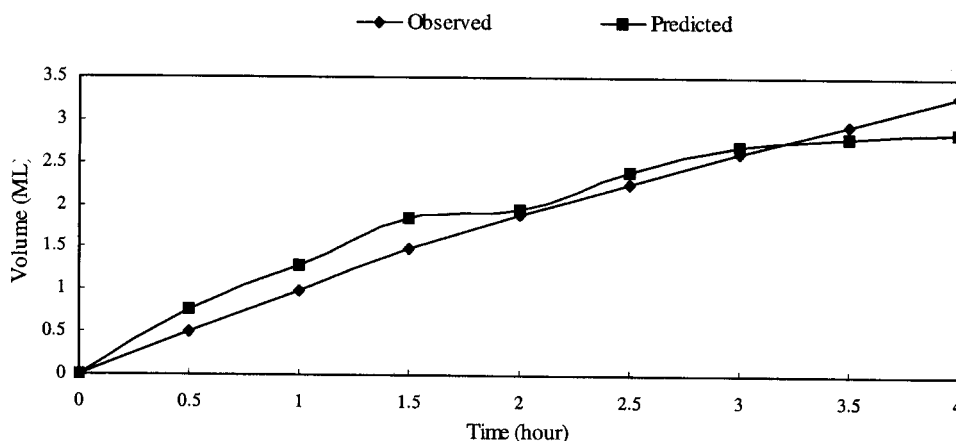


Fig. 14. Water balance during advance phase as predicted by Parlange infiltration equation

of this infiltration model depends on the availability of the soil and infiltration parameters. With the availability of these parameters the user has a choice of selecting either the Parlange infiltration equation or the empirical Kostiakov–Lewis equation. The results indicate that while both these equations do not affect the simulation result significantly in terms of advance time and pattern, the use of Parlange infiltration equation can provide a more accurate water balance approximation. It can also be speculated that the use of Parlange infiltration equation can better represent soil moisture condition as it takes into account of soil moisture into the prediction of infiltration. However such a comparison was not undertaken in this study.

Conclusions

A two-dimensional mathematical computer simulation model was developed to simulate the hydraulic processes involved in the irrigation of contour basin layouts in southeast Australia. The model is based on the zero-inertia approximation of the shallow water flow equations, leading to a two-dimensional advection–diffusion equation including infiltration sink term. The model handles infiltration using either the empirical Kostiakov–Lewis equation or the quasianalytical Parlange equation. The two-dimensional advection–diffusion equation was found to be capable of describing shallow water flow in contour basin irrigation systems accurately over a range of flow and layout configurations. This single equation was solved by the method of characteristics coupled with bicubic splines for rectangular grid discretization.

The computer simulation model was validated against field data collected on a commercial contour basin layout. The variables used for the validation of the model were cumulative wetted area during advance, waterfront advance pattern and volume balance during advance. Modeled and observed cumulative wetted area and waterfront advance patterns were in good agreement barring minor variations which can be ascribed to local undulations caused by sheep tracks and vehicle movement, spatial variation of infiltration and variation in inflow rates which are not included in the present scale of modeling.

Acknowledgments

The authors would like to thank the Land and Water Resources & Development Corporation, Australia for its financial support of this project and the University of Melbourne for providing a student scholarship.

Notation

The following symbols are used in this paper:

- a = infiltration empirical constant;
- b = infiltration empirical constant;
- D_{11}, D_{22}, D_{12} = diffusion coefficients;
- g = acceleration due to gravity (m/s^2);
- H = water surface elevation above datum (m);
- h = water depth (m);
- h_{str} = minimum soil moisture pressure value on wetting cycle (m);
- I_s = volumetric rate of infiltration per unit area (m/s);
- K_i = soil hydraulic conductivity at initial moisture content (m/s);
- K_s = soil hydraulic conductivity at saturation (m/s);
- k = empirical infiltration constant;
- ML = Megaliter ($1,000 \text{ m}^3$);
- n = Manning roughness coefficient;
- q = discharge vector (m^2/s);
- q_x = component of discharge vector per unit width in x direction (m^2/s);
- q_y = component of discharge vector per unit width in y direction (m^2/s);
- S = sorptivity ($\text{m}/\sqrt{\text{s}}$);
- S_f = friction slope;
- S_{fx} = component of friction slope in x direction;
- S_{fy} = component of friction slope in y direction;
- t = time (s);
- t_{op} = intake opportunity time, or time since wetting front is arrived at point or node (s);
- U = advected velocity in x direction (m/s);
- u = velocity in x direction (m/s);
- V = advected velocity in y direction (m/s);
- v = velocity in y direction (m/s);
- x, y = Cartesian coordinates (m);
- x_B, y_B = value of x and y on fixed boundary;
- z_0 = bottom elevation above datum (m);
- Δ = time step (s);
- δ = shape parameter related to conductivity of soil;
- θ = angle between flow direction and x axis;
- θ_i = initial soil moisture; and
- θ_s = soil moisture at saturation.

Subscripts

- B = boundary nodes;
 i, j = location of node on computation grid; and
 x, y = Cartesian coordinates.

References

- Chaudhry, M. H. (1993). *Open-channel flow*, Prentice-Hall, Englewood Cliffs, N.J.
- Clemmens, A. J., Strelkoff, T., and Dedrick, A. R. (1981). "Development of solution for level-basin design." *J. Irrig. Drain. Eng. Div., ASCE*, 107(3), 265–279.
- de Boor, C. D. (1978). *A practical guide to splines*, Springer, New York.
- Edenhofer, J., and Schmitz, G. (1985). "An analytical solution of the infiltration equation for general initial and boundary conditions." *Proc., 21st Congress IAHR*, Melbourne, Australia.
- Glass, J., and Rodi, W. (1982). "A higher order numerical scheme for scalar transport." *Comput. Methods Appl. Mech. Eng.*, 31, 337–358.
- Haverkamp, R., Parlange, J. Y., Starr, J. L., Schmitz, G., and Fuentes, C. (1990). "Infiltration under ponded conditions: 3. A predictive equation based on physical parameters." *Soil Sci.*, 149(5), 292–300.
- Holly, F. M., Jr. and Komatsu, T. (1983). "Derivative approximations in the two-point fourth-order method for pollutant transport." *Proc., Frontiers in Hydraulic Engineering*, ASCE, Reston, Va., 349–355.
- Holly, F. M., Jr., and Preissmann, A. (1977). "Accurate calculation of transport in two dimensions." *J. Hydraul. Div., Am. Soc. Civ. Eng.*, 103(11), 1259–1277.
- Holly, F. M., Jr., and Toda, K. (1985). "Hybrid numerical schemes for linear and nonlinear advection." *Proc., 21st Congress IAHR*, Melbourne, Australia.
- Holly, F. M., Jr., and Usseglio-Polatera, J. M. (1984). "Dispersion simulation in two-dimensional tidal flow." *J. Hydraul. Eng.*, 110(7), 905–926.
- Hume, I. H. (1993). "Determination of infiltration characteristics by volume balance for border check basin." *Agric. Water Manage.*, 23(1993), 23–39.
- Khanna, M., Malano, H. M., Fenton, J. D., and Turrall, H. (2003). "Two-dimensional simulation model for contour basin layouts in southeast Australia. II: Irregular shape and multiple basins." *J. Irrig. Drain. Eng.*, 129(5), 317–325.
- Komatsu, T., Holly, F. M., Jr., Nakashiki, N., and Ohgushi, K. (1985). "Numerical calculation of pollutant transport in one and two dimensions." *J. Hydrosoci. Hydr. Eng.*, 3(2), 15–30.
- Komatsu, T., Ohgushi, K., and Asai, K. (1997). "Refined numerical scheme for advective transport in diffusion simulation." *J. Hydraul. Div., Am. Soc. Civ. Eng.*, 123(1), 41–50.
- Kostiakov, A. V. (1932). "On the dynamics of the coefficient of water percolation in soils and on the necessity for studying it from a dynamics point of view for purposes of amelioration." *Proc., Trans. Sixth Comm. Int. Soc. Soil Sci.*, Moscow, Part A, 17–21.
- Maheshwari, B., and Jayawardarne, N. (1992). "Infiltration characteristics of some clayey soils measured during border irrigation." *Agric. Water Manage.*, 21, 265–279.
- Maheshwari, B., and McMahon, T. A. (1992). "Modeling shallow overland flow in surface irrigation." *J. Irrig. Drain. Eng.*, 118(2), 201–217.
- Parlange, J.-Y., Lisle, I., Braddock, R. D., and Smith, R. E. (1982). "The three-parameter infiltration equation." *Soil Sci.*, 133(6), 337–341.
- Playan, E., Walker, W. R., and Merkle, G. P. (1994a). "Two-dimensional simulation of basin irrigation. I: Theory." *J. Irrig. Drain. Eng.*, 120(5), 837–856.
- Playan, E., Walker, W. R., and Merkle, G. P. (1994b). "Two-dimensional simulation of basin irrigation. II: Applications." *J. Irrig. Drain. Eng.*, 120(5), 857–870.
- Schmitz, G., Haverkamp, R., and Velez, O. P. (1985). "A coupled surface-subsurface model for shallow water flow over initially dry soil." *Proc., 21st Congress IAHR*, IAHR, Melbourne, Australia.
- Schohl, G. A., and Holly, F. M., Jr. (1991). "Cubic-spline interpolation in langrangian advection computation." *J. Hydraul. Eng.*, 117(2), 248–253.
- Shikin, E. V., and Plis, A. I. (1995). *Handbook on splines for the user*, Chemical Rubber Corp., New York.
- Singh, V. (1996). "Computation of shallow water flow over a porous medium." Ph.D. thesis, Indian Institute of Technology, Kanpur, India.
- Singh, V., and Bhallamudi, S. M. (1997). "Hydrodynamic modeling of basin irrigation." *J. Irrig. Drain. Eng.*, 123(6), 407–414.
- Smith, J. (1999). "Draft report on determination of rice soil hydraulic properties by Guelph and Disc permeametry." CSIRO Land and Water, CSIRO, Australia.
- Strelkoff, T. S., Tamaini, A. H. Al-, Clemmens, A. J., and Fangmeier, D. D. (1996). "Simulation of two-dimensional flow in basins and borders." *Presentation at the Proc., ASAE Annual International Meeting*, Phoenix Civic Plaza, Phoenix.
- Zapata, N., and Playan, E. (2000). "Simulating elevation and infiltration in level-basin irrigation." *J. Irrig. Drain. Eng.*, 126(2), 78–84.